

**Modification to the central-cell correction of germanium acceptors**

O. Drachenko,\* H. Schneider, and M. Helm

*Institute for Ion-Beam Physics and Materials Research, Helmholtz-Zentrum Dresden-Rossendorf, D-01314 Dresden, Germany*

D. Kozlov and V. Gavrilenko

*Institute for Physics of Microstructures Russian Academy of Sciences, 603950 Nizhny Novgorod, Russia*

J. Wosnitza

*Dresden High Magnetic Field Laboratory (HLD), Helmholtz-Zentrum Dresden-Rossendorf, D-01314 Dresden, Germany*

J. Leotin

*Laboratoire National des Champs Magnetiques Intenses, 143 av. de Ranguel, F-31432 Toulouse, France*

(Received 10 July 2011; revised manuscript received 7 November 2011; published 19 December 2011)

In this paper, we report a correction to the model potential of the Ga acceptor in germanium, evidenced by high-magnetic-field photoconductivity measurements. We found that under high magnetic fields the chemical shift of the binding energy of Ga acceptors vanishes, contrary to the results given by the generally accepted theory. To fit our data, we found that the central-cell correction should contain a repulsive part (i.e., it must be bipolar), in contrast to the purely attractive screened point-charge potential widely used in the literature.

DOI: [10.1103/PhysRevB.84.245207](https://doi.org/10.1103/PhysRevB.84.245207)

PACS number(s): 72.20.-i, 72.40.+w, 72.80.Cw

**I. INTRODUCTION**

During the past years, germanium has attracted continuously growing attention, stimulated by the fast progress of SiGe electronics, the recent discovery of Ge:Ga superconductivity, and the rising interest in GeMn magnetic semiconductors.<sup>1,2</sup> Consequently, detailed modeling of Ge-based structures again becomes an important task, long after the early era of semiconductor research. In this paper, we discuss peculiarities related to the calculation of the energy states of shallow acceptors (in particular Ga) in germanium.

The energy spectrum of a group-III element (acceptor) replacing germanium in its diamondlike lattice is usually calculated using the Luttinger Hamiltonian and a point-charge potential using the dielectric constant of Ge (note that this model is only valid for distances from the impurity much larger than the lattice constant). This model, however, gives energies that are independent of the chemical nature of the acceptor impurity. On the other hand, experiments show different ionization energies for different group-III elements embedded into the Ge lattice.<sup>3</sup> The element-related dependence of the ionization energy is also called chemical shift.

The chemical shift can theoretically be considered using a central-cell correction, which has its maximum in the vicinity of the impurity center and vanishes on length scales much larger than the lattice constant. Typically, one chooses a point-charge potential with exponential screening:<sup>4-6</sup>

$$\Delta V = -e^2 \frac{\exp(-r/l)}{\kappa_{\text{eff}} r}, \quad (1)$$

where  $\kappa_{\text{eff}} \geq \kappa/(\kappa - 1)$  is the effective permittivity and  $\kappa = 15.36$  is the permittivity of germanium. The experimentally obtained binding energy is then reproduced by varying both fit parameters  $\kappa_{\text{eff}}$  and  $l$ . There exist, however, multiple solutions and the combination of these two parameters is not unique. Additional requirements have to be applied to specify more precisely the choice of the model potential. In this work, we

address the dependence of the chemical shift as a function of magnetic field, which acts as an additional localization factor for the acceptor wave functions. Previously, the chemical shift for donors in GaAs as a function of magnetic field was studied experimentally by Heron *et al.*<sup>7</sup> and theoretically by Jayam and Navaneethakrishnan,<sup>8</sup> who also use the potential (1); however, the magnetic field was limited to 10 T. In the present work, we apply high magnetic fields up to 50 T and argue that a new, alternating-sign, central-cell correction for germanium acceptors has to be used.

**II. EXPERIMENTAL RESULTS**

In this work, we study the photoconductivity of a gallium-doped germanium (Ge:Ga) crystal under high magnetic fields up to 50 T. The sample, with impurity concentration  $N_a - N_d = 2 \times 10^{14} \text{ cm}^{-3}$ , was cut in a  $1 \times 1 \times 1 \text{ mm}^3$  piece. The sample was mounted inside a hemispherical gold-coated cavity and placed in the center of a magnetic-field coil using a variable-temperature insert (VTI). The VTI contains an overmoded optical waveguide (light pipes), a heater, a thermometer, and a magnetic-field sensor.<sup>9</sup> The temperature of the crystal was kept at 2 K in order to minimize the dark current. The magnetic field was aligned in [001] direction. The measurements were performed at Dresden high-magnetic-field laboratory (HLD) at the Helmholtz-Zentrum Dresden-Rossendorf (HZDR) using free electron laser (FEL) excitation. The FEL at HZDR, FELBE, is based on a two-stage superconducting linear accelerator (ELBE—electron linear accelerator of high brilliance and low emittance) with a total energy of up to 40 MeV. The emission wavelength depends on the electron beam energy and the period of the wiggler, and can be tuned from 4 up to 280  $\mu\text{m}$ .<sup>10</sup> A constant 100 mV bias was applied to the gold-coated contacts deposited on the facets perpendicular to the magnetic field. The FEL light of constant intensity was directed into the VTI, and the

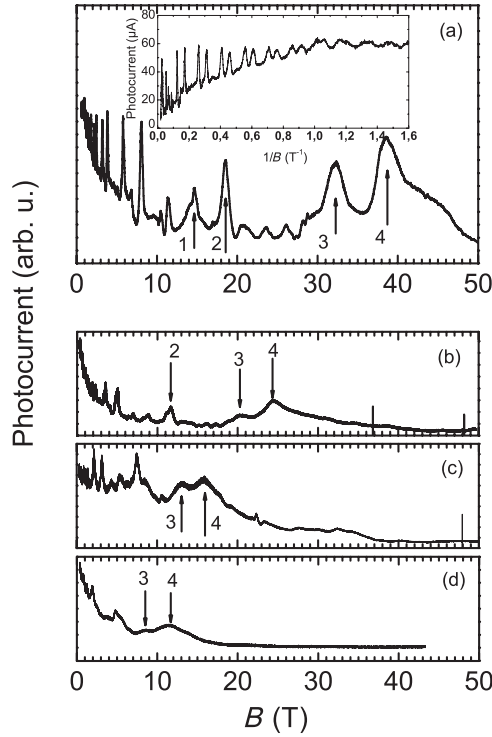


FIG. 1. Photocurrent as a function of magnetic field measured in the Ge crystal illuminated with FEL radiation at (a) 46  $\mu\text{m}$ , (b) 60.5  $\mu\text{m}$ , (c) 75  $\mu\text{m}$ , and (d) 88  $\mu\text{m}$ . The magnetic field is directed along the [001] direction. A 100-mV voltage bias was applied to the facets perpendicular to the magnetic field. The inset of (a) shows the photoconductivity data as a function of reciprocal magnetic field. Vertical arrows point to transitions from the two lowest acceptor states, bound to  $2^1$  and  $1^1$  Landau levels, into the resonant states bound to  $3^1$  (arrows 3 and 4) and  $2^2$  (arrows 1 and 2) Landau levels, respectively (see explanation of the notations in the text).

photocurrent as a function of magnetic field was monitored using a transimpedance amplifier. The experimental setup is described in more detail in Ref. 11 and was recently successfully applied for a number of cyclotron-resonance experiments.<sup>12–16</sup>

Figure 1(a) shows an example of the magnetic field dependence of the photocurrent under FEL excitation at  $\lambda = 46 \mu\text{m}$ . The inset shows the same data plotted versus reciprocal magnetic field. It is clearly seen that the photocurrent shows periodic peaks in the reciprocal magnetic field at low fields ( $B < 10 \text{ T}$ ) (with the period given by the excitation energy) and the peaks are split into two components. These oscillations, previously reported by Zverev and Gantmakher in the late 1970s,<sup>17,18</sup> were attributed to the photoexcitation of the impurity to resonant states bound to the Landau ladder of the light-hole subband, which gives the observed periodicity. The split components of the peaks correspond to transitions into spin-split Landau levels. Due to the large valence-band nonparabolicity, the periodicity is lost at high magnetic fields ( $B > 10 \text{ T}$ ). The full set of data includes photocurrent measurements under FEL excitation at  $\lambda = 46$  to 103  $\mu\text{m}$ . Figures 1(b)–1(d) show the photocurrents under FEL excitations at  $\lambda = 60.5 \mu\text{m}$ ,  $\lambda = 75 \mu\text{m}$ , and  $\lambda = 88 \mu\text{m}$ , respectively. We also performed several measurements

at different values of the applied bias and found no significant effect of this parameter on the oscillation spectra.

### III. THEORETICAL MODEL

In order to analyze the obtained data, we have calculated the energy spectrum of the Ga acceptor in the germanium lattice with applied magnetic field using the effective-mass approximation. The Hamiltonian includes the potential of the impurity ion (point-charge potential), a model potential to account for the chemical shift, and the Luttinger Hamiltonian,  $H_L$ , with magnetic field using the axial approximation,<sup>19</sup>

$$H_L = \hbar\omega_C \text{diag} \begin{pmatrix} A + Ck_z^2 + \frac{3}{4}\kappa \\ B + Dk_z^2 + \frac{1}{4}\kappa \\ B + Dk_z^2 - \frac{1}{4}\kappa \\ A + Ck_z^2 - \frac{3}{4}\kappa \end{pmatrix} + \hbar\omega_C \begin{pmatrix} 0 & Ek_z a & Fa^2 & 0 \\ -Ek_z a^\dagger & 0 & 0 & Fa^2 \\ Fa^{+2} & 0 & 0 & -Ek_z a \\ 0 & Fa^{+2} & Ea^\dagger & 0 \end{pmatrix}, \quad (2)$$

$$\begin{aligned} A &= (\gamma_1 + \gamma_2)(a^\dagger a + 1/2), & B &= (\gamma_1 - \gamma_2)(a^\dagger a + 1/2), \\ C &= (\gamma_1 - 2\gamma_2), & D &= (\gamma_1 + 2\gamma_2), \\ E &= i\gamma_3\sqrt{6}, & F &= \sqrt{3}(\gamma_2 + \gamma_3), \end{aligned}$$

where  $\hbar\omega_C = \hbar eB/m^*c$  is the cyclotron energy,  $m^*$  is the effective mass, and  $\gamma_1$ ,  $\gamma_2$ ,  $\gamma_3$ , and  $\kappa$  are the Luttinger parameters. Operator  $a^\dagger$  in the polar coordinates is given by

$$a^\dagger = \frac{l_C}{\sqrt{2}} \exp(i\varphi) \left( -i \frac{\partial}{\partial \rho} + \frac{1}{\rho} \frac{\partial}{\partial \varphi} + i \frac{\rho}{2l_C^2} \right),$$

where  $l_C = \sqrt{\hbar c/eB}$  is the magnetic length.

The eigenfunctions of the Hamiltonian (2), without taking into account the acceptor impurity, can be written in the following form:

$$G_m^n(k_z, \rho, \varphi, z) = \begin{pmatrix} C_4 \psi_{n-3, m-3}(\rho, \varphi) \\ C_3 \psi_{n-2, m-2}(\rho, \varphi) \\ C_2 \psi_{n-1, m-1}(\rho, \varphi) \\ C_1 \psi_{n, m}(\rho, \varphi) \end{pmatrix} e^{ik_z z}. \quad (3)$$

Here, the  $C_{1, \dots, 4}$  are coordinate-independent coefficients, and

$$\psi_{n, m}(\rho, \varphi) = \frac{1}{l_C} \sqrt{\frac{r!}{(r + |m|)!}} \frac{e^{im\varphi}}{\sqrt{2\pi}} x^{\frac{|m|}{2}} e^{-\frac{x}{2}} L_r^{|m|}(x), \quad (4)$$

where  $x = \frac{\rho^2}{2l_C^2}$ ,  $r = n - \frac{|m|+m}{2}$ ,  $L_r^{|m|}(x)$  are Laguerre polynomials,  $n = 0, 1, 2, \dots$  is the Landau-level (LL) number, and  $m = J_z + 3/2$  is the projection of the angular momentum.

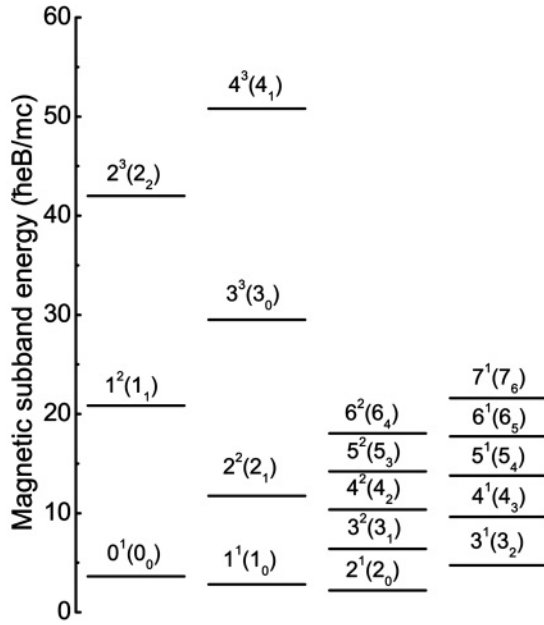


FIG. 2. Energies of the valence-band Landau levels presented in units of the cyclotron energy for free electrons  $\hbar \frac{eB}{m_0 c}$ . Each Landau level is labeled according to the notation explained in the text, while the notations according to Ref. 20 are given in the brackets.

The Hamiltonian (2) has four eigenstates for fixed  $k_z$  and  $n \geq 3$ , three eigenstates for  $n = 2$ , two eigenstates when  $n = 1$ , and, finally, one eigenstate when  $n = 0$ . The hole states can be then expressed by three quantum numbers: the Landau-level number  $n$ , the wave vector  $k_z$ , and the number  $i$  characterizing the sequence of the eigenstate for the given  $n$  and  $k_z$  (since multiple solutions exist when  $n > 0$ ). Therefore, we will use the notation  $n^i$  to identify the magnetic subbands. Note that the lowest magnetic subband is  $2^1$  (equivalent to  $2_0$  using the notations from Ref. 20), which corresponds to the second Landau level.

Figure 2 shows the energies of the magnetic subbands calculated using our method plotted in units of the cyclotron energy for free electrons,  $\hbar eB/m_0 c$ , where  $m_0$  is the free-electron mass. The levels are labeled as explained above, while the notations from Ref. 20 are shown in brackets. We state very good agreement of our results with the data from Ref. 20, with only one exception of the Landau level  $0^1(0^0)$ , which deviates by roughly 15%. This deviation is most likely caused by our simplified axial approximation used in the calculations. This, however, does not influence the following discussion and conclusion.

The wave functions of the acceptor impurity are represented as a linear combination of the eigenfunctions (3),

$$\Psi_m(\mathbf{r}) = \sum_n \int_{-\infty}^{\infty} dk_z C_m(k_z, n) G_m^n(k_z, \rho, \varphi, z). \quad (5)$$

Substituting Eq. (5) to the equation for the effective mass, we get an integral equation for the coefficients of the linear combination. We solve this equation numerically, substituting the integral by a summation with step  $k_z$  much smaller than the inverse Bohr radius. The sum can be truncated for  $k_z$  much larger than the inverse Bohr radius. Additionally, we neglect

components related to higher Landau-level numbers (separated from the ground state by energies much larger than the acceptor ionization energy). Note that the number of Landau levels to be taken into account rises when the magnetic field decreases. It is, therefore, necessary to truncate the calculation at reasonably low fields in order to limit the necessary computation power.

The linear combination (5) includes terms pertaining to different magnetic subbands. If it consists mainly of wave functions of a given magnetic subband, this acceptor state will be bound to that magnetic subband. Corresponding energies of the acceptor can be either negative (localized states) or positive (resonant states) with respect to the ground state  $2^1$  (Fig. 2).

#### IV. RESULTS AND DISCUSSION

When a magnetic field is applied, the ground state of the acceptor, normally fourfold degenerate, splits into four branches corresponding to the four projections of the full momentum  $J_z = \pm 3/2$  and  $J_z = \pm 1/2$ . Figure 3 illustrates how the central-cell correction affects the energies of these states under high magnetic fields. Note that the ionization energy is 9.6 meV when calculated using the axial approximations,<sup>6</sup> 9.8 meV in the spherical approximation,<sup>4</sup> and 10.3 meV taking into account the anisotropy.<sup>21</sup> Since the binding energy of Ga is 11.3 meV<sup>3</sup>, one can assume a chemical shift of the order of  $\sim 1$  meV. The dotted lines correspond to the energies calculated without taking into account the central-cell correction (no chemical shift). The two lowest states correspond to  $J_z = \pm 1/2$  and are bound to the magnetic subbands  $1^1$  and  $2^1$ . The dashed lines show energies of the split states calculated using the central-cell correction (1) in the most localized form ( $\kappa_{\text{eff}} = 1.07$ ,  $l = 3 \text{ \AA}$ ), providing the chemical shift of 1 meV at zero magnetic field. The solid lines correspond to the calculations with the more extended central-cell correction ( $\kappa_{\text{eff}} = 10$ ,  $l = 10 \text{ \AA}$ ), also giving the chemical shift of 1 meV at zero magnetic field. It can be clearly seen that accounting the central-cell correction in the form of Eq. (1) leads to a pronounced increase of the chemical shift (modulus) as a function of magnetic field, which rises up to 4–6 meV when the magnetic field reaches 40 T. More generally, the chemical

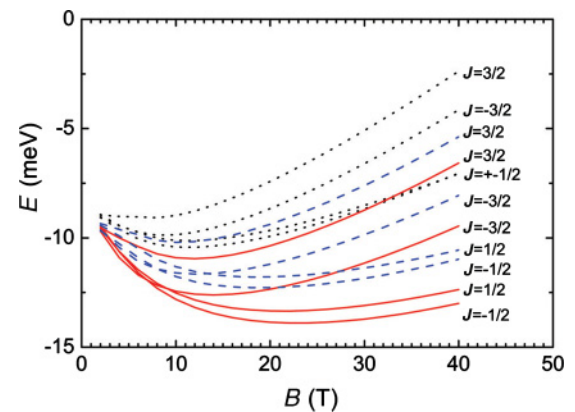


FIG. 3. (Color online) Energies of the ground state of the acceptor as a function of magnetic field, calculated using central-cell correction (1) and  $\kappa_{\text{eff}} = 1.07$ ,  $l = 3 \text{ \AA}$  (solid lines), potential (1) and  $\kappa_{\text{eff}} = 10$ ,  $l = 10 \text{ \AA}$  (dashed lines) and without taking the central-cell correction into account (dotted lines).

shift would rise with magnetic field for any monotonic unipolar (attractive) central-cell correction.

Let us also note that our calculations give a splitting of the two lower acceptor states with  $J_z = \pm 1/2$  of the order of 0.4 meV, which corresponds fairly well to the values reported in Refs. 22 and 23 up to a magnetic field of 10 T. On the other hand, the spectroscopic study of the Zeeman splitting of the Ga acceptor in Ge yields a much lower value (see Ref. 23 and references therein). Therefore, one should expect that at  $T = 2$  K ( $k_B T = 0.18$  meV) both states with  $J_z = \pm 1/2$  should be thermally populated even at fields above 10 T, while the split-off states with  $J_z = \pm 3/2$  are empty. The two lowest acceptor states with  $J_z = \pm 1/2$  are bound to the two lowest hole Landau levels  $2^1$  and  $1^1$ , respectively (Fig. 2).

As we already mentioned, the observed photocurrent oscillations at  $B < 10$  T are periodic in reciprocal magnetic field [see inset of Fig 1(a)], and are related to transitions from the ground acceptor state into the resonant states bound to the two Landau-level ladders (see Fig. 2). At the excitation wavelength of  $\lambda = 46$   $\mu\text{m}$  [Fig. 1(a)], the last pair of the oscillations (at 5.8 T and 8.1 T) is related to transitions into the resonant states bound to the Landau levels of the light holes  $3^3$  and  $1^2$ , respectively (Fig. 2). The next lower Landau subband of light holes  $2^2$  does not have a corresponding pairing level in the second Landau ladder to form a pair of oscillations. Therefore, one or more oscillations of the photocurrent observed above 10 T are expected to be related to transitions into the level  $2^2$  (lines 1–4 in Fig. 1).

Since the sample was installed inside the hemispherical cavity, the light absorbed by the sample contains both polarization components, directed parallel ( $z$  direction) and perpendicular ( $x$ - $y$  plane) to the magnetic field. The selection rules allow dipole transition between adjacent Landau levels ( $\Delta n = \pm 1$ ) for the  $x$ - $y$  polarization, and require conservation of the Landau-level number ( $\Delta n = 0$ ) for  $z$ -polarized light. In the strong magnetic-field limit, similar selection rules apply for transitions between the impurity states. The transition energies between these levels rise quasilinearly with magnetic field (Fig. 4).

Figure 4 summarizes the data obtained in our experiment (symbols). Let us discuss the transitions responsible for the lines labeled 1–4 in Fig. 1. The slopes corresponding to the lines 1 and 2 are 8.7 and 8.1, respectively (in units of  $\hbar e B / m_0 c$ ). The only possible final state for these transitions, as we discussed earlier, is the level  $2^2$  with the energy of  $11.3 \hbar e B / m_0 c$ . For optical transitions with  $x$ - $y$  polarization, the initial state would be  $1^1$  with  $J_z = -1/2$  and the corresponding energy  $2.9 \hbar e B / m_0 c$ . The slope for the transition  $1^1 \rightarrow 2^2$  is then given by  $8.4 \hbar e B / m_0 c$ , which is very close to the experimentally observed one. For  $z$  polarization, the selection rules require conservation of the LL number and  $J_z$ . Since the final state is  $2^2$ , with  $J_z = +1/2$ , the initial state can only be  $2^1$ . However, since the splitting of the ground state with  $J_z = \pm 1/2$  (difference between  $1^1$  and  $2^1$ ) is only a small fraction of meV,<sup>22–24</sup> the transitions  $1^1 \rightarrow 2^2$  and  $2^1 \rightarrow 2^2$  coincide. Similarly, the lines 3 and 4 have the slopes 4.7 and 4.1 in units of  $\hbar e B / m_0 c$ , respectively, which is very close to the energy difference between the levels  $3^2$  and  $2^1$  ( $4.3 \hbar e B / m_0 c$ ).

The solid lines in Fig. 4 show the magnetic-field dependence of the transition energies between the acceptor states

bound to the LLs  $1^1$  and  $2^2$  (lines 1 and 2), as well as to the LLs  $2^1$  and  $3^2$  (lines 3 and 4) calculated according to our model without taking into account the chemical shift. As can be seen, our calculations show good agreement with the experiment without any fit parameters. On the other hand, inclusion of the commonly used central-cell correction (1), as well as any other monotonic unipolar potential, would lead to an enhancement of the chemical shift at high magnetic fields (see Fig. 3). In turn, since the chemical shift affects only the energies of the initial  $s$ -like impurity states, leaving the final  $p$ -like states unaffected,<sup>20</sup> the corresponding transition energies would exhibit a strong blueshift, and, as a consequence, strong deviation of the calculated transition energies from the experiment (see dashed lines in Fig. 4).

Generally speaking, our results give a hint that the chemical shift vanishes at high magnetic fields. Contrary to that, any unipolar attractive central-cell correction would lead to an increase of the chemical shift at high magnetic fields due to the additional magnetic confinement of the carrier wave function around the acceptor ion. The main consequence, therefore, could be that the central-cell correction is not only attractive, but contains a repulsive part. When the magnetic field confines the carrier wave function to this particular region, the chemical shift reduces. Since the chemical shift of all acceptors are usually treated in the same way, we would expect similar behavior for other acceptors in germanium—Al, for example. This, however, should be proven by further experiments.

Let us now consider an example of the central-cell correction that could fit our experimental data. Note, however, that it will require further studies to find the detailed form of the central-cell correction, while it is beyond the scope of the present paper. We only state that the new central-cell correction should contain a repulsive part, since the attractive only potential would lead to monotonic increase of the chemical

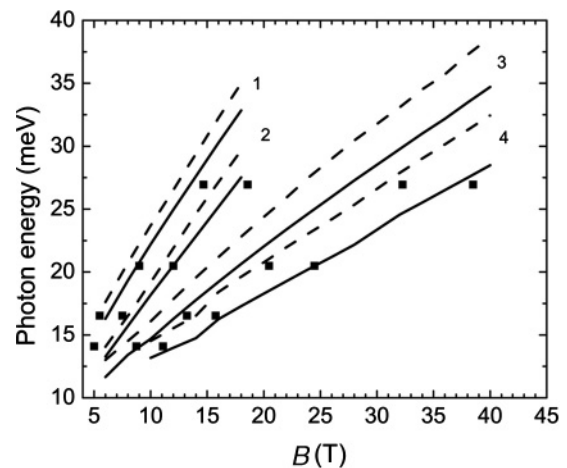


FIG. 4. Summary of the experimentally obtained position of the resonances as a function of magnetic field (symbols). Solid lines show calculations of the transition energies from the two lowest acceptor states bound to the magnetic subbands  $1^1$  and  $2^1$  into resonant states bound to the subbands  $2^2$  and  $3^2$  calculated without taking into account the central-cell correction. Dashed lines correspond to the same transitions calculated using central-cell correction (1) and  $k_{\text{eff}} = 10$ ,  $l = 10$  Å. Numbers indicate corresponding maxima in the photoconductivity spectra (see Fig. 1).

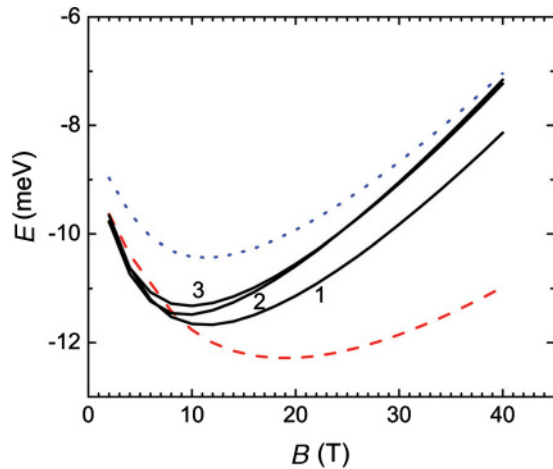


FIG. 5. (Color online) Magnetic-field dependencies of the lowest acceptor-state energy calculated using no central-cell correction (dotted line), with central-cell correction (1) and  $\kappa_{\text{eff}} = 1.07$ ,  $l = 3 \text{ \AA}$  (dashed line), with central-cell correction (6) with the following parameters:  $\kappa_{\text{eff}_1} = 3.84$ ,  $l_1 = 25 \text{ \AA}$ ,  $\kappa_{\text{eff}_2} = 3.07$ ,  $l_2 = 20 \text{ \AA}$  (line 1),  $\kappa_{\text{eff}_1} = 2$ ,  $l_1 = 20 \text{ \AA}$ ,  $\kappa_{\text{eff}_2} = 1.5$ ,  $l_2 = 14 \text{ \AA}$  (line 2), and  $\kappa_{\text{eff}_1} = 5.12$ ,  $l_1 = 30 \text{ \AA}$ ,  $\kappa_{\text{eff}_2} = 3.84$ ,  $l_2 = 25 \text{ \AA}$  (line 3).

shift in a magnetic field, and therefore will fail to fit our experiment.

As a starting point, we tried an alternating-sign central-cell correction in the following (phenomenological) form:

$$\Delta V = -e^2 \left( \frac{\exp(-r/l_1)}{\kappa_{\text{eff}_1} r} - \frac{\exp(-r/l_2)}{\kappa_{\text{eff}_2} r} \right). \quad (6)$$

Figure 5 compares different model potentials. The dotted line shows the results with no central-cell correction, the dashed line represents the central-cell correction (1) with  $\kappa_{\text{eff}} = 1.07$ ,  $l = 3 \text{ \AA}$  as fit parameters, and, finally, the solid lines correspond to the central-cell correction (6) with various fit parameters listed in the caption (lines 1–3). As can be seen, the unipolar central-cell correction leads to a dramatic shift of the lower acceptor state toward higher energies (larger negative

values) when the magnetic field rises above 10 T. On the other hand, one can always find good fit parameters for the bipolar potential (6) to obtain a reduction of the chemical shift at high fields. In addition, the potential (6) also reproduces an increase of the chemical shift at low fields ( $B < 10 \text{ T}$ ) that perfectly matches the behavior reported in Ref. 8.

## V. CONCLUSION

In this work, we have studied oscillations of the photoconductivity in Ge:Ga as a function of magnetic field up to 50 T, when excited with monochromatic FEL radiation. We found these oscillations at  $B < 10 \text{ T}$  to be periodic in reciprocal magnetic field, with the period proportional to the excitation energy. We attribute these oscillations to the optical transitions from the lower acceptor states into resonant states bound to the hole magnetic subbands (Landau levels). At high fields, the periodicity is lost due to the nonequidistant energy spacing between the lowest hole Landau levels. We have developed a theoretical model in order to calculate the acceptor wave functions and energies as a function of magnetic field. We found that accounting for the chemical shift via the commonly used central-cell correction (in the form of a screened point charge) leads to a dramatic increase of the chemical shift at high fields, resulting in a strong deviation of the calculated from the experimentally measured transition energies. In contrast to that, calculations without any central-cell correction show good agreement with the experimental data, which indicates that the chemical shift decreases at high magnetic fields. Decrease of the chemical shift can be attributed to the presence of the repulsive part in the central-cell correction, in contrast to the purely attractive one widely used in literature.

## ACKNOWLEDGMENTS

This work has been partially supported by EuroMagNET II under the EU Contract No. 228043, by DFG projects DR832/2-1 and DR832/3-1, and by Russian Foundation for Basic Research (Grant No. 11-02-00952).

\*o.drachenko@hzdr.de

<sup>1</sup>S. Zhou, D. Burger, A. Muecklich, C. Baumgart, W. Skorupa, C. Timm, P. Oesterlin, M. Helm, and H. Schmidt, *Phys. Rev. B* **81**, 165204 (2010).

<sup>2</sup>T. Herrmannsdörfer, V. Heera, O. Ignatchik, M. Uhlarz, A. Müucklich, M. Posselt, H. Reuther, B. Schmidt, K.-H. Heinig, W. Skorupa, M. Voelskow, C. Wündisch, R. Skrotzki, M. Helm, and J. Wosnitza, *Phys. Rev. Lett.* **102**, 217003 (2009).

<sup>3</sup>E. E. Haller and W. Hansen, *Solid State Commun.* **15**, 687 (1974).

<sup>4</sup>N. O. Lipari, A. Baldereschi, and M. L. W. Thewalt, *Solid State Commun.* **33**, 277 (1980).

<sup>5</sup>J. Bernholc and S. T. Pantelides, *Phys. Rev. B* **15**, 4935 (1977).

<sup>6</sup>V. Ya. Aleshkin, V. I. Gavrilenko, and D. V. Kozlov, *Phys. Status Solidi C* **0**, 680 (2003).

<sup>7</sup>R. J. Heron, R. A. Lewis, P. E. Simmonds, R. P. Starrett, A. V. Skougarevsky, R. G. Clark, and C. R. Stanley, *J. Appl. Phys.* **85**, 893 (1999).

<sup>8</sup>G. Jayam and K. Navaneethkrishnan, *J. Appl. Phys.* **89**, 6198 (2001).

<sup>9</sup>O. A. Mironov, M. Myronov, S. Durov, O. Drachenko, and J. Leotin, *Physica B* **346**, 548 (2004).

<sup>10</sup>J. Wosnitza, T. Herrmannsdörfer, Y. Skourski, S. Zherlitsyn, S. A. Zvyagin, O. Drachenko, H. Schneider, M. Helm, *AIP Conf. Proc.* **1003**, 311 (2008).

<sup>11</sup>O. Drachenko, S. Winnerl, H. Schneider, M. Helm, and J. Leotin, *Rev. Sci. Instrum.* **82**, 033108 (2011).

<sup>12</sup>O. Drachenko, D. V. Kozlov, V. Ya. Aleshkin, V. I. Gavrilenko, K. V. Maremyanin, A. V. Ikonnikov, B. N. Zvonkov, M. Goiran, J. Leotin, G. Fasching, S. Winnerl, H. Schneider, J. Wosnitza, and M. Helm, *Phys. Rev. B* **79**, 073301 (2009).

<sup>13</sup>O. Drachenko, A. Patane, N. V. Kozlova, Q. D. Zhuang, A. Krier, L. Eaves, and M. Helm, *Appl. Phys. Lett.* **98**, 162109 (2011).

- <sup>14</sup>A. Patane, W. H. M. Feu, O. Makarovskiy, O. Drachenko, L. Eaves, A. Krier, Q. D. Zhuang, M. Helm, M. Goiran, and G. Hill, *Phys. Rev. B* **80**, 115207 (2009).
- <sup>15</sup>N. Miura, N. V. Kozlova, K. Dörr, J. Freudenberger, L. Schultz, O. Drachenko, K. Sawano, and Y. Shiraki, *J. Low Temp. Phys.* **159**, 222 (2010).
- <sup>16</sup>O. A. Mironov, M. Goiran, J. Galibert, D. V. Kozlov, A. V. Ikonnikov, K. E. Spirin, V. I. Gavrilenko, G. Isella, M. Kummer, H. von Kanel, O. Drachenko, M. Helm, J. Wosnitzer, R. J. H. Morris, and D. R. Leadley, *J. Low Temp. Phys.* **159**, 216 (2010).
- <sup>17</sup>V. F. Gantmakher and V. N. Zverev, *Sov. Phys. JETP* **46**, 1223 (1977).
- <sup>18</sup>V. N. Zverev, *Sov. Phys. Solid State* **22**, 1921 (1980).
- <sup>19</sup>V. Y. Aleshkin, V. I. Gavrilenko, D. B. Veksler, and L. Reggiani, *Phys. Rev. B* **66**, 155336 (2002).
- <sup>20</sup>J. C. Hensel and K. Suzuki, *Phys. Rev. B* **9**, 4219 (1974).
- <sup>21</sup>A. V. Malyshev, I. A. Merkulov, and A. V. Rodina, *Phys. Rev. B* **55**, 4388 (1997).
- <sup>22</sup>J. Broeckx, *Phys. Rev. B* **43**, 9643 (1991).
- <sup>23</sup>W. O. G. Schitt, E. Bangert, and G. Landwehr, *J. Phys. Condens. Matter* **3**, 6789 (1991).
- <sup>24</sup>P. Fisher, G. J. Takacs, R. E. M. Vickers, and A. D. Warner, *Phys. Rev. B* **47**, 12999 (1993).